

# Experimental Study on Magnesite and Mineral Components Electrostatic Separation Methods

Yunxiao Cao, Zhiqiang Wang, Jinjun Wang, Guofeng Li\*  
Dept. of Electrical Engineering  
Dalian University of Technology  
phone: +86 15524566520  
e-mail: cao\_yunxiao@126.com

**Abstract**—Magnesite is mostly used in fireproofing material, the magnesium oxide advanced functional materials made by magnesite are supporting and leading in the fields of aerospace, aviation, military, metallurgy and environmental protection. However, the impurity content of *Si*, *Ca*, *Fe* and etc. in magnesite is high. There are some technique difficulties for mineral separation now, and it is difficult to achieve efficient separation by existing mature methods, such as floatation. So it cause a lot of accumulated resources waste and environmental pollution problems. In this paper, electrostatic separation is used to separate magnesite and mineral components. The magnesite particle size is grinding to  $20\mu\text{m}$  (D50). And magnesite and mineral components particles are charging by high-voltage corona discharge. Due to the difference of all mineral components' surface electrical property. It could achieve to separate magnesite from impurity minerals. The electrostatic separation platform is built in the experiment. Electric discharge polarity, electric field intensity, electrode position and separation times which all affect the separation efficiency are considered during the experiment process. The experiment results indicate that the element mass fractions of magnesite which dropped in different zones are different obviously. And it's more effective to separate *Si* and *Ca* from magnesite in positive polarity electric field. In conclusion, electrostatic separation method could be used in the separation of magnesite and mineral components. And this paper provides a new way for high efficient and valuable utilization of magnesite.

## I. INTRODUCTION

It is rich in magnesite resources in China, but there's few high-quality magnesite, most of them are low grade. During the exploitation and utilization process of magnesite in China, firstly the top grade magnesite ( $MgO$  more than 46%) is screened and removed to produce refractory material and high purity magnesia. Middle grade magnesite ( $MgO$  43%~46%) is used to manufacture common sintered magnesia, industrial magnesium oxide and activated magnesium oxide. The low grade magnesite ( $MgO$  less than 42%) which is more than 60% of the total reserves is directly stripping in the exploitation process. This causes not only the waste of resources, but also environmental pollution <sup>[1]</sup>.

The main factor restricting the exploitation and utilization of magnesite is high content of calcium, silicate and other impurities in it. It is well known that more than 80% magnesite are used to made refractory lining inside industrial furnaces in the fields of metallurgical, chemical, glass and etc.<sup>[2-5]</sup>. In the roasting process, the  $SiO_2$  from low grade magnesite will form the fusibleness silicate. And this will greatly reduce the strength of the refractory materials.  $CaO$  will become  $CaSiO_3$  when it's in roasting. After cooling the  $CaSiO_3$  will be getting loose separation and refractory materials will breakdown in the same time. Therefore, it is significant for exploitation and utilization of magnesite resource in China that separating and purifying of low grade magnesite and reducing impurities content such as silicon and calcium.

Flotation is a common method for magnesite separation. But the present research about flotation separation is mostly for high grade magnesite, which  $MgO$  content is more than 46%,  $SiO_2$  and  $CaO$  content is less than 2%<sup>[6, 7]</sup>. There's few research about low grade magnesite ( $MgO$  less than 42%) and it is difficult to obtain high quality magnesite concentrate<sup>[8-10]</sup>. Moreover, the flotation is wet processing methods that require water during the processing procedures, and high operation cost is inevitable with the consumption of water. In addition, there are some more problems such as waste water pollution, chemical reagents consumption and dewatering also accompany the wet processing techniques.

Aiming at low exploitation and utilization rate of low grade magnesite, this paper proposed a magnesite and mineral components separation method to remove impurities by high-voltage electrostatic. The electrostatic separation gets more advantage than flotation in both produce costs and environment pollution. In the process of electrostatic separation, charging particles move in different trajectory based on based on their surface charging properties differences. And this is a physical method to realize mineral particles separation. The device structure of electrostatic separator is simple, it is easy maintenance and the production cost is lower. More important is that there's no waste water and dust during separation process, this satisfies the environment requirements.

## II. P EXPERIMENTAL SETUP AND METHODOLOGY

### A. Mechanism of Electrostatic Separation

Magnesite inside mineral mostly exists in the shape of granularity and crystals. Small parts exist in fine granular shape. The main impurity mineral of magnesite are dolomite, calcite, diabase, quartz and etc. Quartz and dolomite exist in the cracks and holes of magnesite, talcum intrude into the micro fracture of magnesite and form fine vein structure. There are some kinds of substance containing iron on the contact edge of magnesite. The rhombohedrons of magnesite have perfect cleavages and it could easily break into small pieces. It always embeds in shape of coarse-particle and its distribution is inhomogeneous in magnesite sample. The valuable mineral and gangues are both easily accomplished to single cleavage. Thus it lays the foundation for successful mineral separation<sup>[11, 12]</sup>.

In this paper, the magnesite will achieve to independent crystal size by smashing and milling. And it makes magnesite and impurity mineral components to accomplish to their single cleavage. The physical properties of low grade magnesite and main mineral components are shown in Table 1.

TABLE 1: PHYSICAL PROPERTIES OF LOW GRADE MAGNESITE AND MINERAL COMPONENTS

| Mineral   | Chemical Formula  | Density /g/cm <sup>3</sup> | Mohs Hardness | Cleavage  |
|-----------|---|----------------------------|---------------|-----------|
| Quartz    | SiO <sub>2</sub>  | 2.22~2.65                  | 7             | imperfect |
| Magnesite | MgCO <sub>3</sub>   | 2.9~3.1                    | 4~4.5         | perfect   |
| Dolomite  | CaMg(CO <sub>3</sub> ) <sub>2</sub>                                     | 2.86~3.2                   | 3~4           | perfect   |
| Calcite   | CaCO <sub>3</sub>   | 2.6~2.8                    | 3             | eminent   |
| Chlorite  | (Mg,Fe <sup>2+</sup> ) <sub>3-x</sub> Al <sub>x</sub> (OH) <sub>6</sub> | 2.6~3.3                    | 2~3           | eminent   |
| Talcum    | 3MgO 4SiO <sub>2</sub> H <sub>2</sub> O                                 | 2.6~2.8                    | 1             | eminent   |

From Table 1, the hardness of carbonate gangues such as magnesite, dolomite and calcite are close, while there are some differences for silicate gangues. The types and contents of silicate gangue in different mineral samples are not same. So it is possible to optimize separation by the method of selective grinding technology. In addition, magnesite, dolomite, calcite, chlorite and talcum are all able to achieve perfect cleavage, only quartz is imperfect cleavage. The Magnesite cleavage plane is shown as Fig. 1.

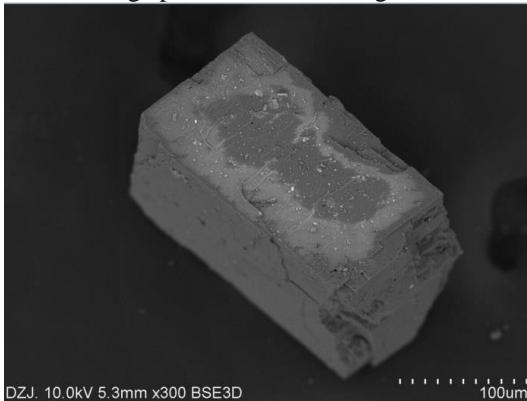


Fig. 1. Magnesite cleavage plane SEM

The magnesite samples are smashed and screened to analyze size distribution. The element content of  $MgO$ ,  $CaO$ ,  $SiO_2$ ,  $Al_2O_3$  and  $Fe$  in different size samples are shown as Fig. 2. It could be known that  $MgO$  content decrease and the impurity content of  $CaO$ ,  $SiO_2$  and  $Al_2O_3$  increase with the size grade of magnesite samples getting lower. It reflects certain selectivity in mineral smashing process.

About the charging mechanism of magnesite particles, there are three practical charging mechanisms in industrial electrostatic separation: conduction charging, triboelectric charging and corona discharge charging<sup>[13-15]</sup>. In this paper, the raw magnesite will first be smashed and milled. So triboelectric charging should be considered. The magnesite particles will be charged by friction between particles or particle and the third material (container, feed box, material outlet and etc.). But there is less charge by triboelectric charging. Thus in this paper, combined charging method (triboelectric and corona charging) is adopted to improve the separation efficiency.

First raw magnesite will be smashed to certain granularity and screened to a certain size range. Then, Magnesite, calcite, quartz and dolomite will be accomplished to their single cleavage by milling equipment. And magnesite and mineral components will be separated in trajectory to separate away from each other based on different charging status in electric

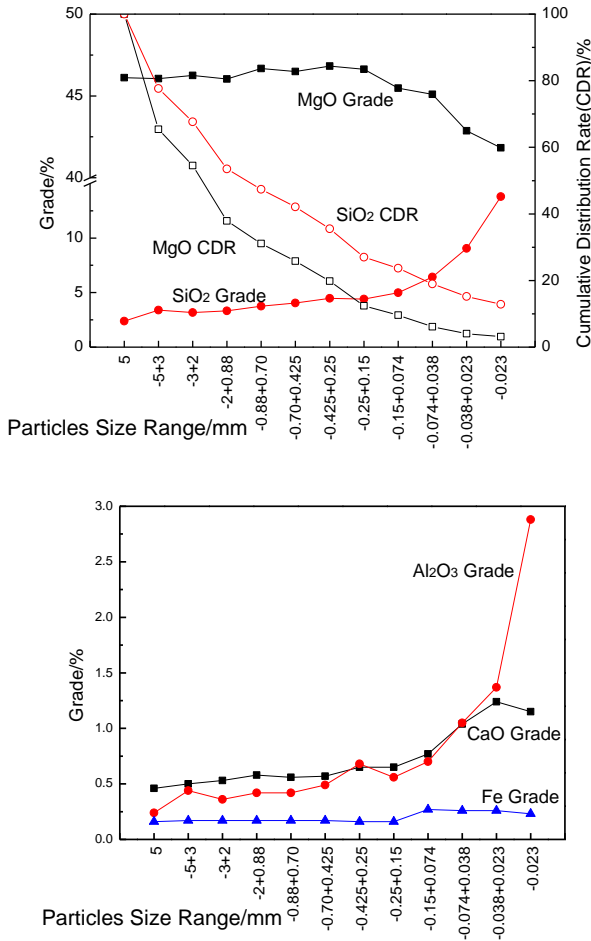


Fig. 2. Size distribution of MgO, CaO, SiO<sub>2</sub>, Al<sub>2</sub>O<sub>3</sub> and Fe in smashed magnesite

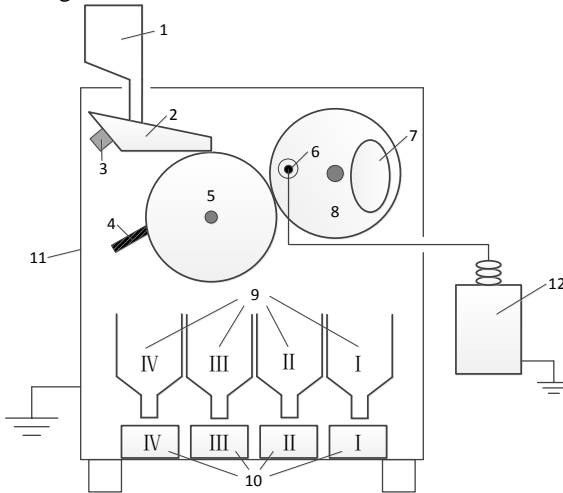
field [16-19]. Permittivity of magnesite and impurity minerals is shown in Table 2. There are differences between the permittivity of various components. And this provides condition for electrostatic separation.

TABLE 2: PERMITTIVITY OF MAGNESITE AND IMPURITY MINERALS

| Number | Minerals  | Permittivity  | Conductivity    |
|--------|-----------|---------------|-----------------|
| 1      | Quartz    | 4.5~6.8       | non- conductive |
| 2      | Talcum    | 5.8, 9.41     | non- conductive |
| 3      | Calcite   | 6.5, 7.8, 9.5 | non- conductive |
| 4      | Magnesite | 7.98          | non- conductive |
| 5      | Dolomite  | 8.45          | non- conductive |

### B. Experiment Setup

Based on the mechanism of electrostatic separation above, an electrostatic separator under DC high-voltage corona discharge is designed in this paper to separate of magnesite and mineral components. The electrostatic separator is built by author's laboratory, and its structure is shown as Fig. 3.



1 Feed box, 2 Material outlet, 3 Vibration motor, 4 Brush, 5 Roller, 6 Discharge electrode, 7 Ellipse electrode, 8 Adjustable dial, 9 Hopper, 10 Collection box, 11 Shell, 12 High-voltage power supply

Fig. 3. The structure diagram of electrostatic separator

The structure of electrostatic separator is relatively compact, including: separator shell, feed box, material outlet, vibration motor, brush, roller, discharge electrode, ellipse electrode, adjustable dial, hopper, collection box and high-voltage power supply. The DC high-voltage power supply is made by author's unit. The voltage value is from 0 to  $\pm 60$  kV and it is adjustable, the power is 120 W. The material of separator shell, feed box, material outlet and roller is metal, and the shell is grounded. The dial, hopper and collection box are all dielectric. The dial can be rotated in  $0\sim 360^\circ$ . The discharge wire and ellipse electrode which installed in the dial could also rotate to change angle. The dial locates in the initial position which the arrow points  $180^\circ$  on the top. The roller connects to motor by belt and the rotation speed of roller is set to 60r/min. The discharge wire connects to high-voltage power supply. The voltage is set from 0 to 25 kV.

The feed box is on the top of separator shell. Material outlet connects to the bottom of feed box. Vibration motor is installed on the slope of material outlet back side. There's roller below material outlet. The roller which connected to shell and brush is on its left side. The brush is used for sweeping roller surface. The adjustable dial is on the right side of roller and it also connects to shell. The discharge wire and ellipse electrode are all installed in the dial. There are four hoppers below roller: hopper IV is located directly below brush, hopper III is located directly below roller, hopper II is located directly below the middle of roller and dial, and hopper I is located below the right side of discharge electrode. The collection boxes are placed below the four hoppers respectively.

### C. Experiment Steps and Phenomenon

First sampling and measurement of the raw magnesite powder which have been smashed and milled. The particle size distribution and mineral composition parameters will be obtained and the data would be as experimental baseline data.

The magnesite powder after measuring will be put into feed box. Then start roller motor, keeping it rotating at low speed and its speed is about 60r/min. After starting vibration motor, the powders will flow out uniformly from material outlet because of vibration and drop on the roller surface. Without high-voltage power supply, the magnesite powders leave the roller and drop into hopper II under the combined centrifugal force and gravity, and then collected by collection box II. A few powders are adsorbed on the roller surface because of triboelectric, swept by brush then drop into hopper IV and collected by collection box IV.

To make the magnesite powders collection more conveniently, first change the position of dial from initial  $180^\circ$  to new  $240^\circ$ , the position is shown as Fig. 4. The discharge electrode will appear corona discharge under DC high-voltage energization. The air around electrode wire will be ionization and the ionized space is full of lots of ions<sup>[20, 21]</sup>. Magnesite powders particles will be charging by free ions after dropping from roller. And due to the ellipse electrode installed on the back side of discharge electrode, the electric field inside separator will be extended<sup>[22]</sup>. Meanwhile, the charging particles in ionization air push the airflow around and form ionic wind under external electric field. About high-voltage corona ionic wind effect, there are some research reports in electrostatic precipitation<sup>[23-25]</sup>. The charging particles move in different trajectory and drop in different hoppers under combined action of electric field force, gravity and ionic wind.

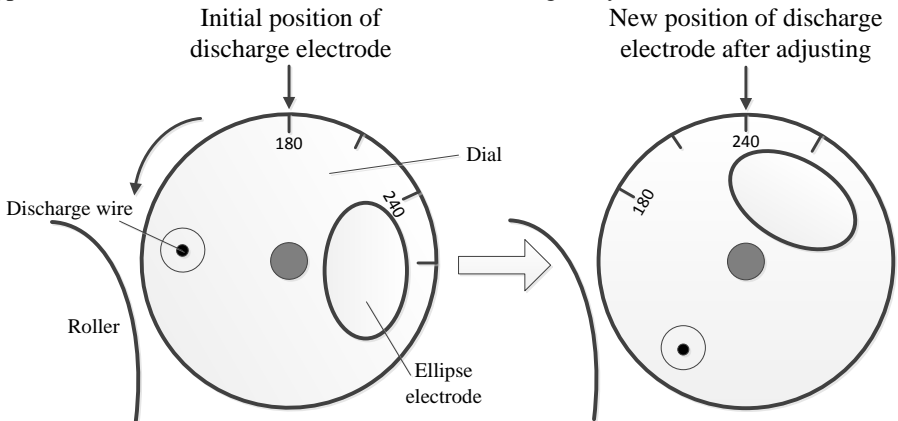


Fig. 4. The position schematic diagram of discharge electrode ( $180^\circ$  to  $240^\circ$ )

Under DC high-voltage energization, the magnesite powders particles which dropped into hopper II will be less obviously than without high-voltage. Only the large particles which not milled completely are collected by collection box II. Most magnesite powders are adsorbed on the roller surface by electric field force, swept by brush then drop into hopper IV. Partial powders are blown by ionic wind which is produced by corona discharge and then drop into hopper III. And a few powders are blown to hopper I by ionic wind in

opposite direction. All the magnesite powders are collected by the four collection boxes below.

Various mineral components surface electric property lead to unequal particle charging status, resulting in different movement trajectory. Magnesite and impurity components will drop into different hoppers along their trajectory.

### III. RESULTS AND DISCUSSION

#### A. Magnesite Sample Size Distribution and Elemental Composition

The magnesite sample in this paper is from Liaoning province of China and it belongs to low grade magnesite. The magnesite sample is smashed and milled to median diameter (D50) 20 $\mu\text{m}$  in the experiment first. The raw magnesite powders particles size distribution is shown in Fig. 5.

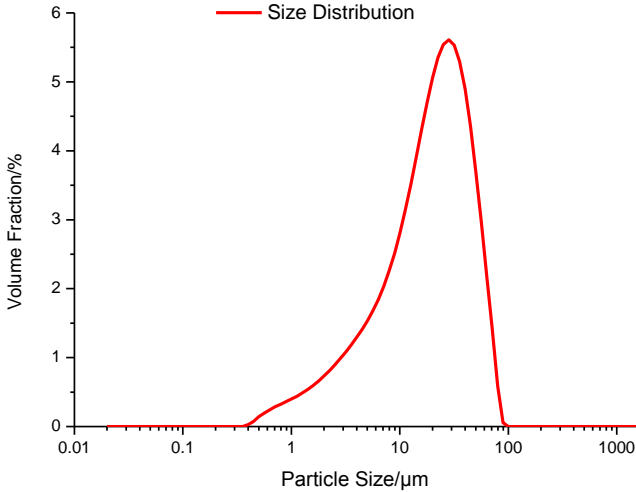


Fig. 5. Raw magnesite powders particles size distribution

Because of the low purity and fine particle size of the magnesite sample in this paper, based on the magnesite cleavage and size grade distribution mentioned above, the mass fraction or content of impurity components in magnesite is very high, and the magnesium grade is low. The raw magnesite powders element composition is tested by X-ray Fluorescence Spectrometric Analysis (XRF). The main element content result is shown in Table 3, such as  $MgO$ ,  $CaO$ ,  $SiO_2$ ,  $Fe_2O_3$  and  $Al_2O_3$ .

TABLE 3: THE MAIN ELEMENT OF MAGNESITE MASS FRACTION RESULT

| Main Components                | Content /% |
|--------------------------------|------------|
| CaO                            | 45.8774    |
| MgO                            | 27.9253    |
| SiO <sub>2</sub>               | 18.6756    |
| Al <sub>2</sub> O <sub>3</sub> | 4.1948     |
| Fe <sub>2</sub> O <sub>3</sub> | 2.0789     |

### B. Single Separation Result Analysis

For the single separation, the discharge electrode is in  $240^\circ$  position, and the separator energized with negative DC high-voltage. Under low voltage (less than 10 kV), the magnesite powders are mostly dropped into hopper II because there's no corona discharge. When the voltage rises to 10 kV, the corona occurs and the magnesite particles movement gets more obviously with voltage value increasing. After 25 kV, the discharge electrode starts to appear spark. So the voltage value set to 25 kV. The separation phenomenon just like what mentioned in chapter 2.3. The raw magnesite powder particles are flowing into the electric field after the roller rolling. And the particles are dropping into different hoppers and collected by four collection boxes respectively. Sampling from different collection boxes and analyzing the main components ( $MgO$ ,  $CaO$ ,  $SiO_2$ ,  $Al_2O_3$  and  $Fe_2O_3$ ) of mineral particles. The result is shown as Fig. 6.

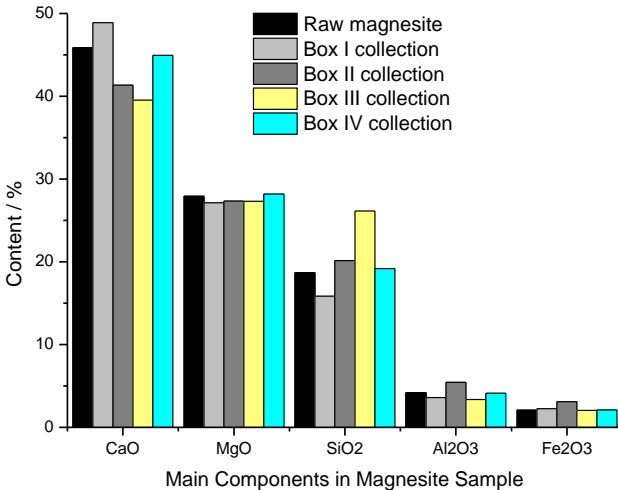


Fig. 6. The main components content changing in four collection boxes after single separation

For collection box I, the content of  $CaO$  is more than raw magnesite powder obviously, it is 48.88%. The  $SiO_2$  content is less than raw magnesite, the content is 15.85%. And the other components are almost same with raw magnesite.

For collection box II, the  $CaO$  content is 41.35% and it's less than raw magnesite. The content of  $SiO_2$ ,  $Al_2O_3$  and  $Fe_2O_3$  are all more than the raw one. They are 20.15%, 5.44% and 3.09% respectively.

For collection box III, the most obviously change is  $SiO_2$ , its content is 26.14%, and this is much more than raw magnesite. And the content of  $CaO$  is the least in the four collection boxes, the content is 39.53%.

For collection box IV, the content of all the main components are very small different with raw magnesite except the  $MgO$  which is a little more than the raw one.

The result indicates that after single electrostatic separation, the main components content of magnesite powder in four collection boxes are different from each other and the raw magnesite because of different mineral surface electric property.

### C. Multiple Separation Result Analysis

Based on the single separation result, it indicates that electrostatic separation could be used to separate impurity components from magnesite powders, such as *Ca*, *Si*, *Al* and *Fe*. Especially for the separation of *Si*, *Al* and *Fe*, and this mostly reflect in the magnesite powders which collected by box II and III. Therefore, for the multiple separation experiment, the mineral components (*Si*, *Al* and *Fe*) content are mainly considered which collected in box II and III respectively. And the element mass fraction changing is studied to analyze the separation effect and efficiency.

Three times separation experiment are done in succession. After each separation, sampling and measurement of the element mass fraction of the mineral powders in box II and III, and then remove the mineral powders which collected in box II and III. The rest powders are used in the next separation experiment. The impurity element content changing is shown as Fig. 7.

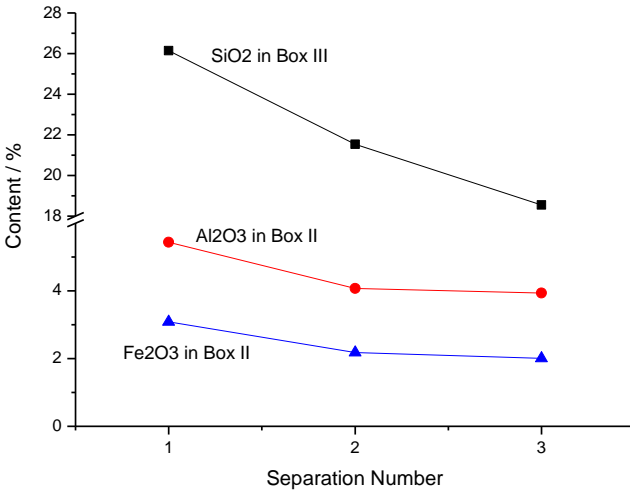


Fig. 7.  $SiO_2$ ,  $Al_2O_3$  and  $Fe_2O_3$  content changing after multiple separations

The result indicates that the content of impurity (*Si*, *Al* and *Fe*) get lower with the increasing number of separation experiments. After three separations, the  $SiO_2$  content in box III decrease from 26.14% (single separation) to 18.55%, and the content of  $Al_2O_3$  and  $Fe_2O_3$  which collected in box II is reduced from 5.44% and 3.09% (single separation) to 3.94% and 2.01% respectively. Combined with the single separation result and analysis of the mineral powders which collected in four collection boxes respectively, it could be got the conclusion that the content of *Si*, *Al* and *Fe* would decrease for the whole magnesite powders after multiple separation.

### D. Positive High-voltage Separation Result Analysis

In this paper, the positive DC high-voltage power supply is also used in the experiment to test the electrostatic separation effect and efficiency. After the test, the result indicates that the  $SiO_2$  content in collection box III is much more than that under negative energization. The main components mass fraction data of collection box III of two electric discharge polarities are shown in Table 4.

TABLE 4: THE MAIN COMPONENTS CONTENT OF COLLECTION BOX III FOR TWO POLARITIES

| Main Components                | Content / %   |          |          |
|--------------------------------|---------------|----------|----------|
|                                | Raw Magnesite | Negative | Positive |
| CaO                            | 45.8774       | 39.5281  | 33.4480  |
| MgO                            | 27.9253       | 27.3035  | 26.8970  |
| SiO <sub>2</sub>               | 18.6756       | 26.1412  | 29.2967  |
| Al <sub>2</sub> O <sub>3</sub> | 4.1948        | 3.3517   | 6.1547   |
| Fe <sub>2</sub> O <sub>3</sub> | 2.0789        | 2.0591   | 2.1945   |

As energized with positive high-voltage, the separation effect for  $SiO_2$  is better than negative discharge polarity and the content of  $CaO$  is much less than negative power supply. So it's more effective to separate  $Si$  and  $Ca$  under positive energization.

#### IV. CONCLUSION

(1) It will reflect certain selectivity for low grade magnesite in smashing and milling process. The content of  $MgO$  will be decreasing with the smashing product size getting smaller. On the contrary, the impurity content of  $CaO$ ,  $SiO_2$ ,  $Al_2O_3$  and  $Fe_2O_3$  will be increasing in the same condition.

(2) The main gangues in low grade magnesite mineral are quartz and dolomite. The symbiotic relationship is close between quartz and magnesite. And the quartz is hard to achieve perfect cleavage. The physical and chemical properties of dolomite are very close to magnesite. So it need to multipurpose use surface electrical property and density distribution to accomplish separation. Because of the full commutate quality of iron mineral, the limonite will drop into the hopper by gravity force, so more  $Al_2O_3$  (5.44%) and  $Fe_2O_3$  (3.09%) are collected in box II.

(3) For single separation, the result indicates that the high-voltage electrostatic could be used in separation impurity components from magnesite powders sample. In high-voltage electrostatic field, different mineral components surface electric property lead to different particle charging status, resulting in different movement trajectory. The element mass fractions of mineral powders which are in different collection boxes are not same with each other. The  $CaO$  content in box I increase from 45.87% to 48.88%. In box II, the  $Al_2O_3$  and  $Fe_2O_3$  increase from 4.19% to 5.44% and 2.08% to 3.09% respectively. The changes of  $SiO_2$  in box III is obvious so much, which increases from 18.68% to 26.14%.

(4) Three most obvious changes of impurities,  $SiO_2$ ,  $Al_2O_3$  and  $Fe_2O_3$ , are mostly studied for multiple separations. The result indicates that the content of impurities get lower with the increasing number of separation. For box II, the  $Al_2O_3$  decrease from 5.44% to 3.94% and  $Fe_2O_3$  decrease from 3.09% to 2.01%, and for box III, the  $SiO_2$  is reduced from 26.14% to 18.55%. That means the impurities content of  $Si$ ,  $Al$  and  $Fe$  would decrease for the whole magnesite powders after multiple separation.

(5) For single separation under positive energization, the  $SiO_2$  content in box II increase from 26.14% (under negative energization) to 29.30%, and  $CaO$  content decrease from 39.53% (under negative energization) to 33.45%. The result indicates that it's more effective to separate  $Si$  and  $Ca$  under positive energization than negative.

## REFERENCES

- [1] Chen J, Honaker R. Dry separation on coal-silica mixture using rotary triboelectrostatic separator[J]. *Fuel Processing Technology*, 2015, 131: 317-324.
- [2] Gence N, Özdağ H. Surface properties of magnesite and surfactant adsorption mechanism[J]. *International journal of mineral processing*, 1995, 43(1): 37-47.
- [3] Fu D, Wang Y, Peng J, et al. Mechanism of extracting magnesium from mixture of calcined magnesite and calcined dolomite by vacuum aluminothermic reduction[J]. *Transactions of Nonferrous Metals Society of China*, 2014, 24(8): 2677-2686.
- [4] BUKOVSKÝ V. Yellowing of newspaper after deacidification with methyl magnesium carbonate[J]. *Restaurator*, 1997, 18(1): 25-38.
- [5] Guo M, Jones P T, Parada S, et al. Degradation mechanisms of magnesia-chromite refractories by high-alumina stainless steel slags under vacuum conditions[J]. *Journal of the European Ceramic Society*, 2006, 26(16): 3831-3843.
- [6] Raza N, Zafar Z I, Najam-ul-Haq M. Utilization of formic acid solutions in leaching reaction kinetics of natural magnesite ores[J]. *Hydrometallurgy*, 2014, 149: 183-188.
- [7] Yao J, Yin W, Gong E. Depressing effect of fine hydrophilic particles on magnesite reverse flotation[J]. *International Journal of Mineral Processing*, 2016, 149: 84-93.
- [8] Del Valle-Zermeño R, Formosa J, Aparicio J A, et al. Reutilization of low-grade magnesium oxides for flue gas desulfurization during calcination of natural magnesite: a closed-loop process[J]. *Chemical Engineering Journal*, 2014, 254: 63-72.
- [9] Hu W, Feng N, Wang Y, et al. Magnesium production by vacuum aluminothermic reduction of a mixture of calcined dolomite and calcined magnesite[J]. *Essential Readings in Magnesium Technology*, 2014: 121-125.
- [10] Yuna Z, Guocai Z. A technology of preparing honeycomb-like structure MgO from low grade magnesite[J]. *International Journal of Mineral Processing*, 2014, 126: 35-40.
- [11] Jones M H, Wilson B W. Rapid method for the determination of the major components of magnesite, dolomite and related materials by X-ray spectrometry[J]. *Analyst*, 1991, 116(5): 449-452.
- [12] Mucci A, Morse J W. Auger spectroscopy determination of the surface-most adsorbed layer composition on aragonite, calcite, dolomite, and magnesite in synthetic seawater[J]. *American Journal of Science*, 1985, 285(4): 306-317.
- [13] Paluch I R, Sartor J D. Thunderstorm electrification by the inductive charging mechanism: I. Particle charges and electric fields[J]. *Journal of the Atmospheric Sciences*, 1973, 30(6): 1166-1173.
- [14] Matsusaka S, Maruyama H, Matsuyama T, et al. Triboelectric charging of powders: A review[J]. *Chemical Engineering Science*, 2010, 65(22): 5781-5807.
- [15] Chang J S, Lawless P A, Yamamoto T. Corona discharge processes[J]. *Plasma Science, IEEE Transactions on*, 1991, 19(6): 1152-1166.
- [16] Dascalescu L, Mizuno A, Tobazón R, et al. Charges and forces on conductive particles in roll-type corona-electrostatic separators[J]. *Industry Applications, IEEE Transactions on*, 1995, 31(5): 947-956.
- [17] Dascalescu L, Morar R, Iuga A, et al. Charging of particulates in the corona field of roll-type electroseparators[J]. *Journal of Physics D: Applied Physics*, 1994, 27(6): 1242.
- [18] Kelly E G, Spottiwood D J. The theory of electrostatic separations: A review part II. Particle charging[J]. *Minerals Engineering*, 1989, 2(2): 193-205.
- [19] Yanar D K, Kwetkus B A. Electrostatic separation of polymer powders[J]. *Journal of Electrostatics*, 1995, 35(2): 257-266.
- [20] H. J. White. Particle charging in electrostatic precipitation[J]. *AIEE Transactions*, 1951, 70(2): 1186-1191.
- [21] K. Parker. Electrical operation of electrostatic precipitators[M]. London: The Institution of Engineering and Technology, 2003: 21-26.
- [22] Dascalescu T Z L, Touhami S, Miloudi M, et al. Corona-assisted plate-type electrostatic separation process for granular plastic wastes[C]//*Industry Applications Society Annual Meeting, 2015 IEEE. IEEE, 2015: 1-6.*
- [23] Nur M, Bonifaci N, Denat A. Ionic wind phenomenon and charge carrier mobility in very high density argon corona discharge plasma[J]. *Journal of Physics: Conference Series*, 2014, 41(12): 495-498.
- [24] Zhang Y, Liu L J, Chen Y, et al. Characteristics of ionic wind in needle to ring corona discharge[J]. *Journal of Electrostatics*, 2015, 15(74): 15-20.
- [25] Colas D F, Ferret A, Pai D Z, et al. Ionic wind generation by a wire-cylinder-plate corona discharge in air at atmospheric[J]. *Journal of Applied Physics Pressure*, 2010, 30(6): 103-108.